Computer Methods in Biomechanics and Biomedical Engineering
Vol. 14, No. 2, February 2011, 183–193

Taylor & Francis
Taylor & Francis Group

Implementation of asymmetric yielding in case-specific finite element models improves the prediction of femoral fractures

Loes C. Derikx[a]*, Roeland Vis[a], Timo Meinders[b1], Nico Verdonschot[a,c2] and Esther Tanck[a3]

[a]*Orthopaedic Research Laboratory, Radboud University Nijmegen Medical Centre, P.O. Box 9101, 6500 HB Nijmegen, The Netherlands;* [b]*Department of Mechanics of Forming Technology, Faculty of Engineering Technology, University of Twente, P.O. Box 217, 7500 AE Enschede, The Netherlands;* [c]*Laboratory of Biomechanical Engineering, Faculty of Engineering Technology, University of Twente, P.O. Box 217, 7500 AE Enschede, The Netherlands*

(*Received 2 June 2010; final version received 19 November 2010*)

Although asymmetric yielding in bone is widely shown in experimental studies, previous case-specific non-linear finite element (FE) studies have mainly adopted material behaviour using the Von Mises yield criterion (VMYC), assuming equal bone strength in tension and compression. In this study, it was verified that asymmetric yielding in FE models can be captured using the Drucker–Prager yield criterion (DPYC), and can provide better results than simulations using the VMYC. A sensitivity analysis on parameters defining the DPYC (i.e. the degree of yield asymmetry and the yield stress settings) was performed, focusing on the effect on bone failure. In this study, the implementation of a larger degree of yield asymmetry improved the prediction of the fracture location; variations in the yield stress mainly affected the predicted failure force. We conclude that the implementation of asymmetric yielding in case-specific FE models improves the prediction of femoral bone strength.

Keywords: bone strength; prediction; finite element modelling; yield asymmetry; metastatic bone disease

Introduction

The pathological fracture risk is one of the most impeding complications for patients suffering from metastatic bone disease in weight-bearing long bones (Van der Linden et al. 2003). The metastatic lesion weakens the bone locally, and has often a dominant effect on the risk of fracture. Lesions with an expected low-fracture risk are treated conservatively with radiotherapy for pain (Hoskin 2003), or, if widespread disease is present, with systemic chemotherapy (Harvey 1997), hormonal therapy (Harvey 1997) and/or bisphosphonates (Body 2003; Hoskin 2003), whereas high-risk lesions are treated surgically in order to stabilise the bone surrounding the lesion. In the case of femoral metastases, the surgical procedures can have a significant impact on the quality of life of cancer patients, since they are associated with high morbidity and mortality rates and an intensive period of rehabilitation. Therefore, surgeons are critical in their judgement towards the risk of fracture and the health of the patient before they choose to operate on the patient. In the event that it is decided not to operate on a patient with a high-risk lesion, a pathological fracture may occur spontaneously which dramatically reduces the quality of life of the patient. Thus, the reliable prediction of the femoral fracture risk is important for the treatment of cancer patients with bone metastases. The currently available clinical methods to determine the femoral fracture risk have shown to be unable to clearly discern the two risk categories. These methods are mainly based on lesion characteristics derived from conventional X-rays, and poorly estimate the fracture risk of low risk lesions. In addition, they greatly over-predict the number of high-risk lesions, resulting in large numbers of surgical overtreatment (Mirels 1989; Hipp et al. 1995; Body 2003; Van der Linden et al. 2004). Therefore, there is an urgent need for a better predictor of the femoral fracture risk in cancer patients suffering from bone metastases.

Case-specific non-linear finite element (FE) models have shown to be promising in the prediction of the individual fracture risk both in intact and in affected femora (Keyak 2001; Keyak, Kaneko, Rossi, et al. 2005; Keyak, Kaneko, Tehranzadeh, et al. 2005; Keyak et al. 2007; Bessho et al. 2007; Lenaerts and van Lenthe 2009; Orwoll et al. 2009; Tanck et al. 2009). In contrast to the currently available clinical methods, these models account for the individual bone strength and allow for the application of specific loading patterns, which has considerably improved the accuracy of the femoral fracture risk prediction as compared with predictions by clinical experts (Tanck et al. 2009).

Previous non-linear FE models adopted post-yield material behaviour, using the Von Mises yield criterion (VMYC; Keyak 2001; Keyak, Kaneko, Tehranzadeh, et al. 2005; Tanck et al. 2009). This yield criterion assumes that the ultimate bone strength under tension equals the ultimate strength under compression. However, it is

*Corresponding author. Email: l.derikx@orthop.umcn.nl

ISSN 1025-5842 print/ISSN 1476-8259 online

DOI: 10.1080/10255842.2010.542463
http://www.informaworld.com

commonly known from the studies on bone material that compressive yield strength ($\sigma_{y,c}$) is higher than the tensile yield strength ($\sigma_{y,t}$; Keaveny et al. 1994; Kopperdahl and Keaveny 1998; Morgan and Keaveny 2001; Kaneko et al. 2003; Bayraktar, Morgan, et al. 2004). Asymmetric yielding can be captured by using the pressure-dependent Drucker–Prager yield criterion (DPYC), which was already utilised in bone specimens on the micro-scale level (Mullins et al. 2009).

To our knowledge, asymmetric yielding using the DPYC has been applied in a few macro-scale femur FE studies before (Bessho et al. 2007, 2009), in which the parameters defining the DPYC were based on limited experimental data. For example, an ultimate yield stress ratio of 80% was implemented, as found in one study on trabecular bone (Keaveny et al. 1994) and another on cortical bone (Kaneko et al. 2003). However, the literature shows variable data in terms of the degree of yield asymmetry. Ratios of tensile to compressive yield stress range from 54% (Kaneko et al. 2003) to 91% (Kopperdahl and Keaveny 1998). Hence, implementing yield asymmetry to predict the fracture risk of metastatic bones requires a sensitivity analysis of the FE predictions to these variable degrees of asymmetrical failure.

Therefore, the aim of the study presented in this paper was twofold. First, it was verified that asymmetric yielding in bone could be captured by the DPYC and can provide better results than the commonly used VMYC. Second, a sensitivity analysis was performed, in which we focused on variations in the parameters defining asymmetric yielding, based on the ranges reported in the literature, and the subsequent effect on bone failure, in terms of failure force and failure location. On the basis of these results, we defined the best parameter settings for using the DPYC in the prediction of the femoral bone strength by case-specific non-linear FE models.

Methods

Mechanical experiments

Two pairs and two single fresh-frozen cadaveric human femora (age 63–81; 2 women, 2 men; institutional approval obtained) were cleaned from soft tissue. The two single femora were kept intact. In the paired femora, one was kept intact, whereas in the other femur artificial metastatic lesions were created by drilling holes through the cortex of the femora. The location and size of these lesions were discussed with experienced physicians in order to resemble clinical appearance of bone metastases in cancer patients. In one bone, we created a 40-mm lesion in the medial shaft of the femur, whereas in the other femur we drilled two 30-mm holes in the anterior shaft, located at the level of the lesser trochanter, and in the distal shaft of the femur, respectively.

All femora were mechanically loaded to failure. For a detailed description of the setup of the mechanical experiments, the reader is referred to Tanck et al. (2009). All femora were embedded in polymethylmethacrylate (PMMA) bone cement for adequate fixation in the experimental setup. The FE models were exactly aligned with the experimental setup, in order to identically apply the load in the two setups. For that purpose, a Roentgen stereophotogrammetric analysis (RSA) was performed. All femora were equipped with 24 tantalum RSA pellets. Subsequently, imaging data were collected. First, quantitative CT (QCT) images were acquired (ACQSim, Philips, Eindhoven, The Netherlands). The following settings were used: 120 kVp, 220 mAs, slice thickness 3 mm, pitch 1.5, spiral and standard reconstruction, in-plane resolution 0.9375. As the ultimate goal of this study is to enable true case-specific bone strength predictions in patients suffering from bone metastases, we used a rather coarse resolution for the QCT-scans, common to current clinical practice in radiotherapeutic departments. The specimens were scanned in a water basin, which was positioned atop a solid calibration phantom containing tubes with 0, 50, 100, and 200 mg/calcium hydroxyapatite (Image Analysis, Columbia, KY, USA). Hounsfield units (HUs) found in the tubes of the calibration phantom were related to their known calcium equivalent values (ρ_{QCT}). On the basis of these relations, grey values in the CT scans were converted to calcium equivalent densities. Second, for the purpose of RSA analysis, a stereo X-ray was taken from the femora while positioned in their experimental setup (Figure 1(A)). Movement of the femora was restricted to rotation around the dorsoventral axis by using a distal-bearing ball and a sliding hinge. A single-limb stance-type loading pattern was applied by means of a hydraulic MTS machine, using a plastic cup (Ø 30 mm, polyoxymethylene, Delrin®). The femora were loaded from 0 N until failure, with a load rate of 10 N/s. During the experiments, failure forces and displacements were recorded.

FE model

The QCT images served as a basis for the geometrical and mechanical properties of the FE model. By segmenting the CT images (Mimics 11.0, Materialise, Leuven, Belgium) we retrieved the 3D surface geometry of the model, which in turn was converted into a solid mesh (Patran 2005 r2, MSC Software Corporation, Santa Ana, CA, USA) using four-noded tetrahedral elements (mean edge length ~2 mm). Using the phantom's calibration data, HUs in the CT scan were automatically converted to ρ_{QCT} values using the Dicom Toolkit software package, developed in-house. Subsequently, these element-specific ρ_{QCT} values were converted into ash densities (ρ_{ash}) and bone material properties, respectively (Keyak, Kaneko, Tehranzadeh,

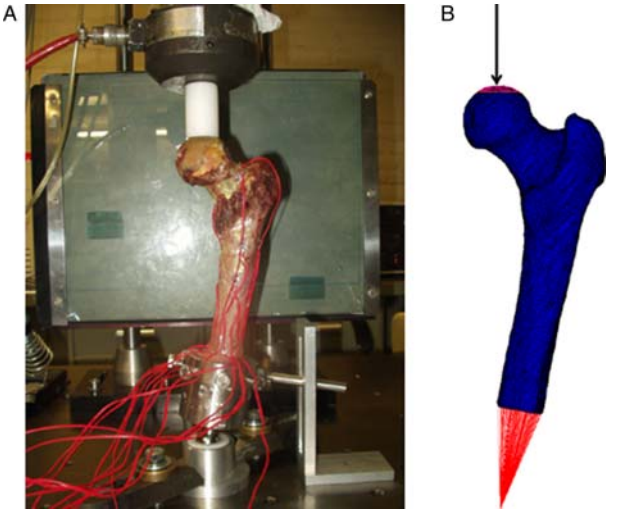

Figure 1. The methodological setup in this study. (A) In the mechanical experiments, the femora were placed in a hydraulic MTS machine and loaded until failure. Movement of the femur was restricted to rotation around the dorsoventral axis by means of a distal bearing ball and a sliding hinge. (B) The FE model exactly mimicked the boundary conditions of the experimental setup.

et al. 2005). Next, a non-linear isotropic post-yield material behaviour was adopted, according to Keyak, Kaneko, Tehranzadeh, et al. (2005).

The orientation of the model was based on the RSA analysis. The RSA pellet positions in the FE model, retrieved from the CT scans, were projected onto the positions of the RSA pellets in the X-rays. The resulting transformation matrix was applied to the FE model. In this way, the FE model was oriented exactly in the experimental position. The distal PMMA fixation and the distal ball bearing in the experiments were simulated by means of two bundles of high stiffness springs, only allowing rotation around the dorsoventral axis. Application of the single-limb stance-type loading pattern mimicked the experimental setup; a displacement-driven load (0.1 mm per increment) was applied via a cup (Ø 30 mm) on the head of the femur (Figure 1(B)). Post-yield material behaviour was not implemented in the surface elements underneath this cup in order to prevent distortion artefacts as a result of the load application. FE simulations were performed using MSC software (MSC.MARC2007 r1, MSC Software Corporation, Santa Ana, CA, USA). The total reaction force in the loading direction was calculated; the maximum value of this force defined failure of the FE model. Displacements were calculated in a reference node on the femoral head, underneath the centre of the loading cup. The fracture location and fracture surface in the FE models were determined by elements that had undergone plasticity, i.e. elements that had passed the softening phase in the post-yield material behaviour.

Sensitivity analysis on the parameters defining the DPYC

In previous FE studies that were related to the prediction of the femoral bone strength, the VMYC was applied (Keyak 2001; Keyak, Kaneko, Tehranzadeh, et al. 2005; Tanck et al. 2009), assuming equal bone strength under tension and compression (Figure 2, left section). In this study, we first implemented the post-yield material behaviour using the VMYC and used these predictions as a reference. Second, we adopted asymmetric yield behaviour using the DPYC (Figure 2, right sections) and performed a sensitivity analysis on the parameters defining the DPYC. In Figure 2 (middle section), a 2D graphical representation of the DP yield envelope is presented. The horizontal axis represents the hydrostatic pressure

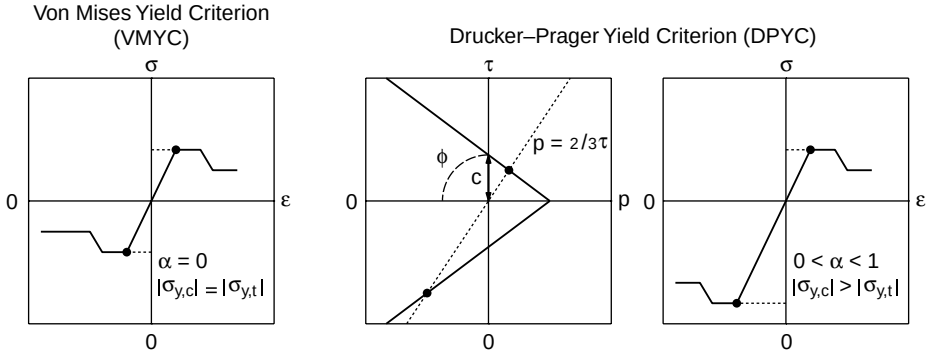

Figure 2. Schematic overview of post-yield material behaviour. Left Panel: The VMYC, using post-yield material behaviour according to Keyak, Kaneko, Tehranzadeh et al. (2005). This criterion assumes equal bone strength under tension and compression. Middle Panel: A 2D representation of the Drucker–Prager yield envelope. The intersection points of the yield envelope and the dashed line indicate the yield points in uni-axial tension (upper right) and uni-axial compression (lower left). The yield points in this figure correspond to the yield points in the right panel. Right Panel: The DPYC, which accounts for yield asymmetry, i.e. the absolute value of the tensile yield stress is smaller than that of the compressive yield stress.

Table 1. Literature overview of yield asymmetries.

	Bayraktar Morgan et al. (2004)	Keaveny et al. (1994)	Kopperdahl and Keaveny (1998)	Morgan and Keaveny (2001)	Kaneko et al. (2003)
Type of bone	Trabecular	Trabecular	Trabecular	Trabecular	Cortical
Origin of specimens	Human	Bovine	Human	Human	Human
Anatomic site	Femur	Tibia	Vertebrae	Femur	Femur
Tensile yield stress (MPa)	82.80	15.60	1.75	10.93	83.90
Compressive yield stress (MPa)	133.60	21.30	1.92	17.45	153.00
Degree of asymmetry (α)	0.135	0.089	0.027	0.133	0.168

axis, for which it holds:

$$p = \frac{1}{3}(\sigma_1 + \sigma_2 + \sigma_3), \tag{1}$$

where p is the pressure and σ_1, σ_2 and σ_3 are the stresses in principal direction. Under uni-axial stress in the σ_1 direction at yielding, this formula reduces to

$$p = \frac{1}{3}\sigma_{\text{yield}}. \tag{2}$$

The vertical axis represents the shear stress axis, for which the following applies:

$$\tau_{\max} = \frac{1}{2}\sigma_{\text{yield}}, \tag{3}$$

where $\tau_{\max}$ is the maximum shear stress. By combining the relationships as defined in Equations (2) and (3), we can derive the following relationship between p and τ:

$$p = \frac{2}{3}\tau. \tag{4}$$

This relationship is depicted by the dashed line in Figure 2 (middle panel). The two points of intersection of the DP yield surface with the dashed line correspond to the yield points in compressive and tensile direction in the 1D stress–strain curve (Figure 2, right panel), when the specimen is loaded in one of the principal directions. Thus, the shape of the DP yield surface directly relates to the degree of asymmetry and is defined by the friction angle φ and the cohesion factor c (Figure 2, middle section):

$$\sin(\varphi) = \frac{3\alpha}{\sqrt{(1 - 3\alpha^2)}}, \tag{5}$$

$$c = \frac{\sigma}{\sqrt{3(1 - 12\alpha^2)}}, \tag{6}$$

where σ is the tensile yield stress and α is the degree of asymmetry in tensile and compressive yield strength:

$$\alpha = \left(\sigma_{y,c} - \sigma_{y,t}\right)/[\left(\sigma_{y,c} + \sigma_{y,t}\right) \times \sqrt{3}], \tag{7}$$

where $\sigma_{y,c}$ is the compressive yield stress and $\sigma_{y,t}$ is the tensile yield stress. From these equations and Figure 2, it should be clear that the position of the cone along the hydrostatic pressure axis depends on both α and the yield stress (σ), whereas the width of the cone is only determined by α. A larger difference in tensile and compressive bone strength results in a larger value of α, which in turn leads to an increase in c and φ, and thus in a wider yield envelope.

In this study, the sensitivity analysis on α was based on results from experiments and experimentally calibrated FE modelling as reported in the literature (Table 1). The specimens used in these studies were rather diverse in terms of the species and the anatomic site they originated from. In order to diminish an eventual effect of these inconsistencies, we used data from experiments with human trabecular bone only. From these data, a minimum, an average and a maximum value of α were calculated, i.e. $\alpha = 0.027$, 0.082 and 0.135. The stress–strain curves for the three different values of α are given in Figure 3 (bottom section). Note that for these cases the choice was made to keep the compressive yield stress equal in all the three graphs.

Previously, the VMYC was used to describe the post-yield material behaviour of bone (Keyak, Kaneko, Tehranzadeh, et al. 2005). On the basis of the compressive yield stress found in experiments, the VM yield stress (VMσ_y) was calculated per element using

$$\sigma_y = 102 \times \rho_{\text{ash}}^{1.8}. \tag{8}$$

We based the sensitivity analysis on yield stress on these fitted VM results. For the implementation of this post-yield material behaviour with the DPYC, we first let the MARC-FE package calculate the yield stresses in tension and compression with its default settings, resulting in a more negative compressive yield stress (DP $\sigma_{y,c}$) and a less positive tensile yield stress (DP $\sigma_{y,t}$) as compared with the VM simulations and experimental results. This case was defined as DEFAULT (Figure 3, upper section). Next, the DP $\sigma_{y,c}$ was equated to the VM σ_y, resulting in a less positive DP $\sigma_{y,t}$ as compared with the VM σ_y. This case was defined as the compression-equated case (COMP_EQ; Figure 3). Although the VM σ_y was validated against compressive experiments, the calculated yield stress was applied in both tension and compression, because the VMYC assumes symmetric yielding. Hence, in the second

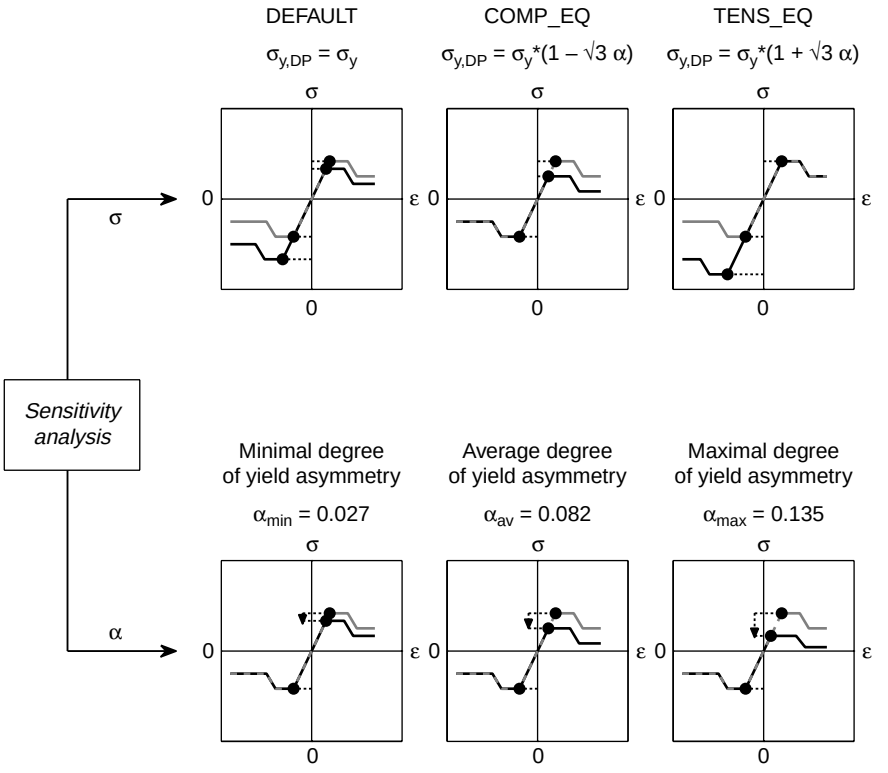

Figure 3. Overview of the different parameter settings in the sensitivity analysis on post-yield material behaviour, implemented using the DPYC. For the variations in fitting the yield stress (upper panels), the DP yield stress was not equated to the VM yield stress (DEFAULT), equated to the VM yield stress in compression (COMP_EQ), or in tension (TENS_EQ). For the variations in the degree of yield asymmetry (lower panels), the minimal and maximal values of α were based on yield asymmetry data reported in the literature (Kopperdahl and Keaveny 1998; Bayraktar, Morgan et al. 2004), and the average value was calculated as the mean of these two values.

variation, DP $\sigma_{y,t}$ was fitted to VM σ_y, resulting in a more negative DP $\sigma_{y,c}$ as compared with the VM simulations. We defined these conditions as the tension-equated case (TENS_EQ; Figure 3).

Data analyses

The effects of implementing variable yield asymmetries on bone failure were evaluated in terms of fracture location and failure forces. The fracture locations predicted by the FE model at the moment of failure were qualitatively compared with the fracture locations in the experiments.

The accuracy of the FE strength predictions was evaluated by determining the correlation and the linear regression equations between the actual experimental bone strength and the bone strength predicted by the FE model. More specifically, using SPSS (SPSS 16.02, SPSS Inc., Chicago, IL, USA), the coefficient of determination (R^2), the regression coefficient and intercept were calculated. In addition, we compared the mean, minimum and maximum relative differences between the experimental failure force and the failure forces predicted by the FE models for every parameter setting. The FE model adopting the VMYC served as a reference. The results of the sensitivity analysis of the two DP parameters were compared to this VM simulation in a descriptive manner.

Results

Fracture location

In the four bones without artificial metastases, the prediction of the fracture location improved by the implementation of the DPYC. For example, in Figure 4, the fracture location in one of the experiments, the VM simulation and the DP simulation (with a maximal α and the yield stress equated in compression, COMP_EQ) are shown. For two of the intact bones, a considerable improvement in the prediction of the fracture line was seen, whereas in the remaining two bones a more subtle effect of the use of yield asymmetry was found. In the experiments, intertrochanteric and transcortical fractures were seen. This pattern was reasonably reproduced when the DPYC was used but was not reproduced in the VM simulations. More specifically, the VM simulations mainly predicted subcapital fractures, whereas the implementation of the DPYC resulted in a fracture that was located more towards the greater and lesser trochanter. It was

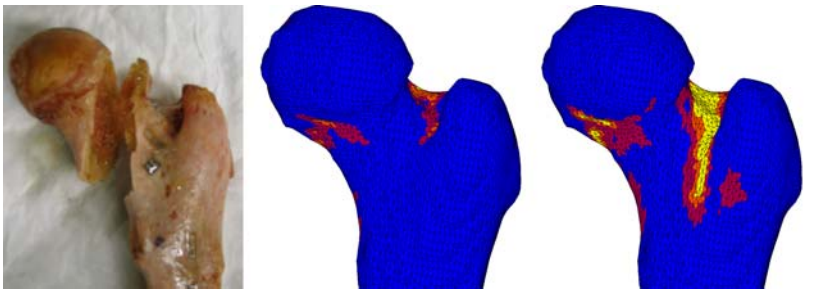

Figure 4. Location of fracture in the experiment, FE simulation using the VMYC and FE simulation using the DPYC. The fracture location was better predicted in the DP simulation than in the VM simulation.

found that a larger degree of yield asymmetry, i.e. higher values of α, better predicted the fracture line. Variations in the yield stress did not have an effect on the location of the fracture line.

In the bones with artificial metastases, the VM simulations correctly predicted the fracture locations through the lesions. The same fracture location was found when using the DP yield criterion.

Failure force

The implementation of the DPYC improved the prediction of the ultimate bone strength. Due to the small number of specimens in this study, no significant differences were found between the different parameter settings in this study. However, we found a number of interesting trends in this study. The predictions by the FE models using the VMYC were already fairly good ($R^2 = 0.91$, slope $= 0.92$, intercept $= -629$), but the correlations between the actual and predicted failure forces in the DPYC simulations were higher (R^2 values ranged from 0.91 to 0.94; Figure 5(A)). The variations in the yield stress had a large effect on the predicted failure force. The DEFAULT simulations best approached the actual failure forces with high correlations ($0.91 < R^2 < 0.94$) and slopes that were close to 1 ($0.93 <$ slope < 1.01; Figure 5). Equating the DP compressive yield stress to the VM yield stress (COMP_EQ) resulted in high correlations as well ($R^2 = 0.94$ in all the three setting of α) and slopes ranging between 0.77 and 0.86 (Figure 5). In the same vein, fitting the DP tensile yield stress to the VM yield stress (TENS_EQ) showed R^2 in between 0.91 and 0.94, whereas the slopes ranged between 0.95 and 1.25 (Figure 5). The intercepts of the regression equations ranged from -459 to -116, but were never significantly different from zero.

The mean, minimum and maximum absolute differences (in %) between the predicted and experimental failure forces are depicted in Figure 6. The simulations with a DEFAULT yield stress condition showed the lowest absolute differences compared with the experiments. From these results, and the finding that a larger degree of yield asymmetry improves the prediction of fracture locations, the best settings to implement asymmetric yielding in the FE prediction of the femoral bone strength were defined as a maximal degree of asymmetry and a default yield stress (i.e. no fit to the VM yield stresses under either compression or tension).

Furthermore, the combined variations in both α and yield stress had a synergetic effect on the failure forces. For example, the effect of variations in the yield stresses was larger when implemented with a larger degree of asymmetry (Figure 7).

In addition, we found that the effect of the sensitivity analysis was dependent on the ultimate strength of the bone (Figure 8). In the weakest bone, the range of predicted failure forces was 1000 N, whereas in the strongest bone this range increased to almost 5000 N, which in both cases approximated 50% of the failure force.

Discussion

The aim of this study was to verify that asymmetric yielding in bone can be captured by the DPYC and can provide better results than the commonly used VMYC. In addition, we performed a sensitivity analysis on the parameters defining asymmetric yielding. We studied the subsequent effect on bone failure, in terms of failure force and failure location, and defined the best possible settings for using the DPYC in the prediction of the femoral bone strength by case-specific non-linear FE models.

Although the highest correlations between predicted and actual failure forces were found when using the DPYC, all FE models in this study were able to adequately predict the femoral bone strength. FE predictions of the failure force were related to the experimental failure force with coefficients of determination ranging between 0.91 and 0.94. These results are in line with previously reported work (R^2 values ranging between 0.83 (Keyak, Kaneko, Tehranzadeh, et al. 2005) and 0.96 (Bessho et al. 2009)).

The variation in the degree of yield asymmetry mainly affected the fracture location, whereas variations in yield

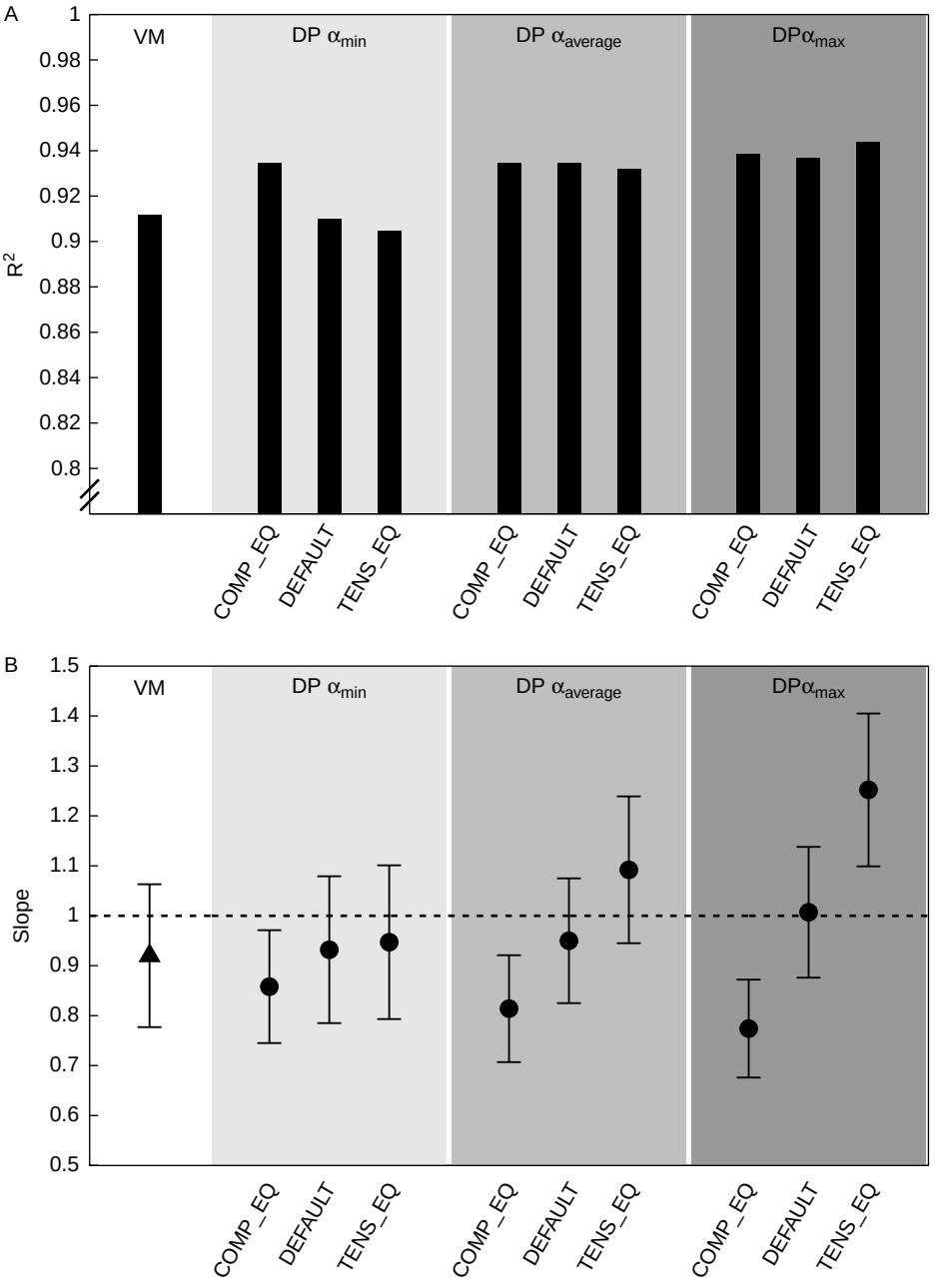

Figure 5. The accuracy of the FE strength predictions. (A) We compared the bone strength predicted by the FE model with the actual experimental bone strength in terms of the correlation, and (B) the slopes (with 95% confidence intervals) of the linear regression equations.

stress had a marked effect on the failure force. In the femora without metastatic lesions, fracture locations were better predicted by models using a large yield asymmetry. These results may be explained as follows. In studies based on the experiments with human bone, it was shown that compressive bone strength is higher than the tensile strength (Keaveny et al. 1994; Kopperdahl and Keaveny 1998; Morgan and Keaveny 2001; Kaneko et al. 2003; Bayraktar, Morgan, et al. 2004); thus, the use of a symmetric yield criterion such as the VMYC would consequently either overestimate the tensile bone strength or underestimate the compressive bone strength. In either case, the failure prediction by an FE model using the VMYC will be biased towards failure under compression. Under single-limb stance-type loading, as utilised in this study, the proximal–lateral femoral neck is assumed to be mainly loaded in tension, whereas the distal–medial part is mainly loaded in compression. Using a symmetric yield criterion would, therefore, lead to fractures that initiate in the distal–medial parts of the femoral neck, as predicted

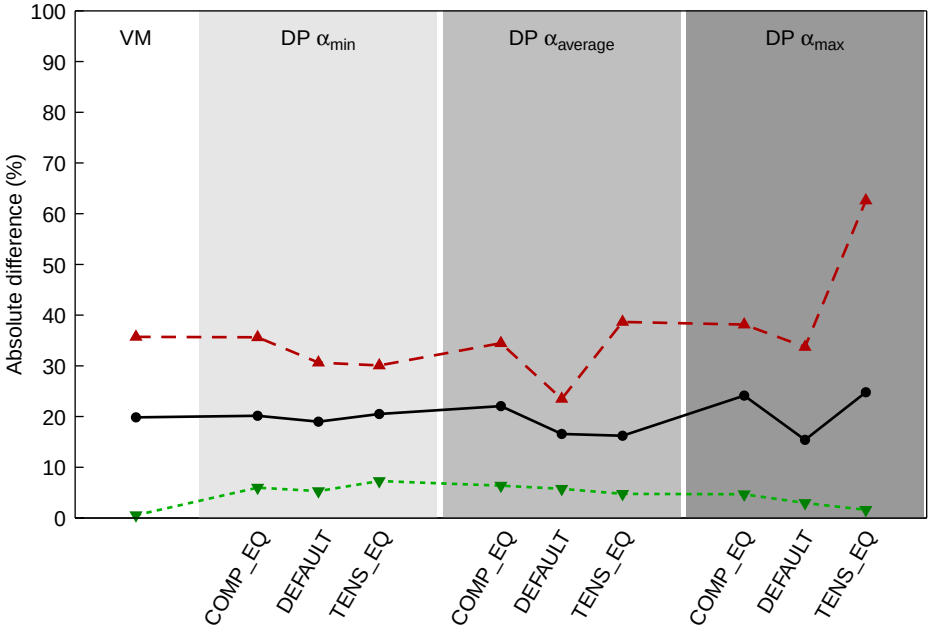

Figure 6. The mean (black circles), minimum (green triangles) and maximum (red triangles) absolute differences (in %) between the experimental failure force and the failure forces predicted by the FE models for every parameter setting.

in the VM simulations. The use of an asymmetric yield criterion can account for this bias towards failure under compression. Indeed, when using the DPYC, the FE model predicted more failure in elements that were loaded under tension, and the resulting fracture locations were more in line with the experimental fracture locations. In the femora with artificial lesions, we found virtually no differences in fracture location predicted in VM simulations and DP simulations. The artificial lesions were located in the medial and anterior femoral shaft. Under single-limb stance-type loading, these areas are loaded primarily under compression, so that the effect of implementing yield asymmetry is reduced. In addition, by drilling holes that mimicked artificial metastases, the femoral cortex was interrupted. As a result, the large forces directed along the shaft of the femur had to be redirected through much weaker, trabecular bone. Consequently, extensive failure in the elements surrounding the artificial lesion was found. This effect might have overruled the more subtle effect of the implemented yield asymmetry. In order to verify this hypothesis, more femora with artificial lesions in other locations (e.g. the lateral shaft or the femoral neck) should be tested.

The variations in the yield stress had a large effect on the failure forces predicted by the FE models. On the basis of the current set of specimens, the best possible failure force prediction was obtained when using a yield stress not fitted to the VM yield stresses in tension nor in compression (DEFAULT), in combination with the largest degree of yield asymmetry.

The combined variations in the degree of yield asymmetry and yield stress had a synergetic effect on the failure force. On the element level, the variations in yield stress gradually led to an increase in the cohesion factor, in which COMP_EQ < DEFAULT < TENS_EQ. Furthermore, a larger degree of yield asymmetry (a larger value of α) increases both the friction angle (φ) and the cohesion factor (c) on the element level. A larger friction angle and cohesion factor result in a wider yield envelope and thus in a larger effect of the hydrostatic pressure on the yield stress. Thus, the increase in predicted bone strength as a result of variations in the degree of asymmetry and yield stress depends on the 3D stress distribution, which implies that the effect on the global bone strength is sometimes difficult to comprehend.

In addition, on the global level, the effect of variable DP parameters was dependent on the ultimate bone strength. Variations in α and yield stress affect the ratio between the tensile and compressive yield strengths. Therefore, absolute difference between tensile and compressive yield strength is larger in FE models with stronger elements. Again, this effect on the bone strength is dependent on the 3D stress distribution, such that the effect on the global strength is not so straightforward.

The results in this study are in line with those in previous studies investigating the implementation of asymmetric yielding on the micro-level. Mullins et al. (2009) showed that micro-level FE models implementing the DPYC better predicted bone failure parameters retrieved by nanoindentation than FE models using the VMYC. Furthermore, Keaveny and co-workers developed validated

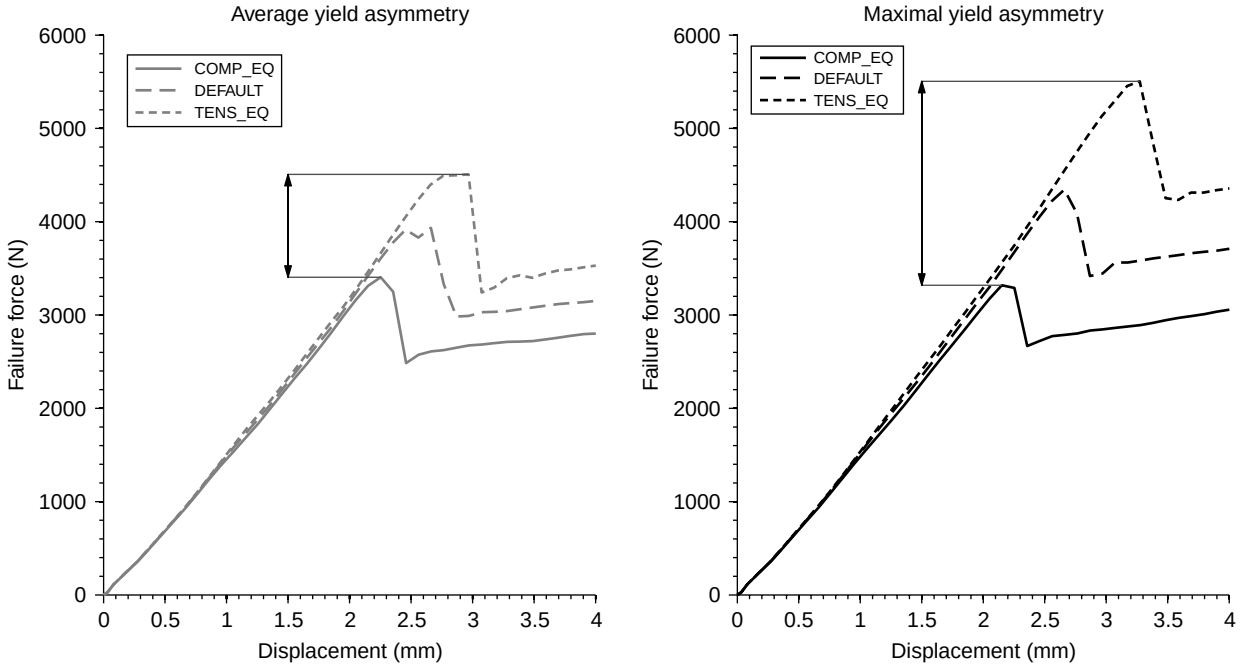

Figure 7. Force–displacement curves for combinations of variations in the yield asymmetry and the yield stress, which had a synergetic effect on the predicted failure forces.

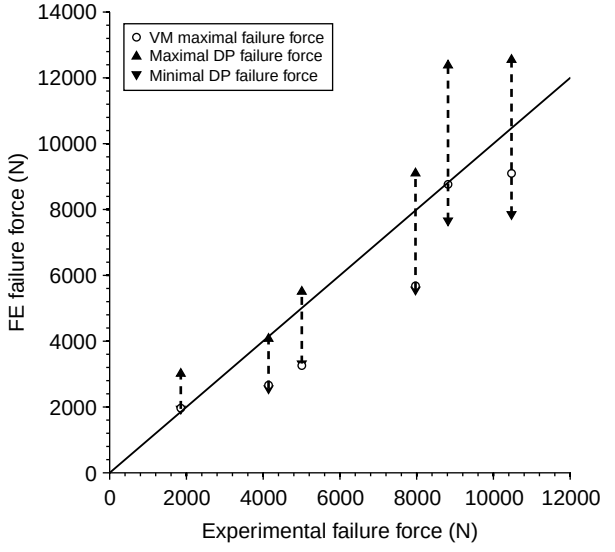

Figure 8. The sensitivity to the various parameter settings of the asymmetric yield criterion is dependent on the global bone strength. For every femur, the largest and smallest failure forces predicted by models using the DPYC as well as the predictions by the models using the VMYC are depicted. In the weakest bone, the range of predicted failure forces was 1000 N, whereas in the strongest bone this range increased to almost 5000 N, which in both cases approximated 50% of the failure force.

micromechanical FE models using an asymmetric yield criterion (Niebur et al. 2000; Bayraktar, Morgan, et al. 2004) or a multiaxial yield surface (Bayraktar, Gupta, et al. 2004), with which they were better able to capture experimentally measured yield behaviour of both human and bovine bone. In contrast, Keyak and Rossi (2000) performed a sensitivity analysis on global femoral FE models using various yield criteria. Their results showed that the implementation of complex yield behaviour (e.g. asymmetric yielding) worsened the prediction as compared with the use of symmetric, simpler yield criteria. However, they did not consider the implementation of the DPYC, which, as this study shows, has the capacity to improve the predictions relative to experimental measurements.

A few limitations of this study should be considered. First, it should be noted that we only used four intact femora and two femora with metastatic lesions, which is from a statistical point of view a small population. With this number of specimens, there is a lack of statistical power to qualify the one parameter setting above and beyond another one, i.e. no statistically significant differences were found between the various parameter settings. However, as a result of the three variations in α, three variations in the yield stress and one VM simulation, we ran 60 non-linear simulations in total. In order to confine calculation time, we used a limited number of specimens. In future work, the best possible parameters found in this study will be applied to, and validated in, a larger population. Furthermore, we congregated the failure data of intact and metastatic femora. Since the failure process of these two groups is fairly different, this might affect the homogeneity of the sample and, therefore, the interpretation of the results. However, in a previous study of our group (Tanck et al. 2009), we found that the accuracy of the predictions by the FE model further increased when

separately considering the results in the two groups. Obviously, analyses on a large number of intact and metastatic femora are needed to confirm these results.

Second, in the intact femora, the predicted fracture locations did not perfectly overlay on the fracture locations as found in the experiments. The FE models predicted the fracture locations more towards the subcapital region, whereas the experimental fractures were located more in between the greater and lesser trochanter. This may be due to the fact that mechanical anisotropy was not implemented in this model. It has been shown that a significant part of the variation in bone strength is explained by the variable trabecular orientation of the bone (Lenaerts and van Lenthe 2009). According to Wolff's law, trabeculae in the femoral head and neck orient towards the physiological loading direction. More specifically, two different trabecular patterns can be distinguished, (i.e. a compressive band and a tensile band), which traverse in the centre of the femoral head (Kyle et al. 1995). The trabeculae in these bands are stronger when loaded in the preferential direction. Thus, by implementing anisotropy, elements in the subcapital region become more resistant to single-limb stance-type loading, being a daily physiological loading condition. Consequently, elements located more towards the greater trochanter might fail earlier, and the fracture location might be further improved. However, it is very difficult to retrieve local anisotropy parameters *in vivo* (Lenaerts and van Lenthe 2009), but taking into account these trabecular bands maybe a first step towards implementation of anisotropy in the FE models.

Finally, we used a single-limb stance-type loading pattern, allowing us to exactly mimic the experiments. However, with this loading type, we could not cover complex loading conditions in daily activities. Although FE models incorporating this simple loading configuration have shown to be successful, more sophisticated loading patterns might further improve the accuracy of the FE predictions. Therefore, future work will focus on the application of muscle forces and hip joint contact forces determined by musculoskeletal models in order to apply such complex loading configurations to the FE model.

In conclusion, in this study we further developed our subject-specific non-linear FE model. By implementing a large degree of yield asymmetry using the DPYC, we showed an improvement in the prediction of bone strength as well as in the prediction of the fracture location.

Acknowledgements

This project has been funded by the Dutch Science Foundation NWO-STW (NPG.06778), the Furlong Research Charitable Foundation and Stichting Anna Fonds.

Notes

1. Email: v.t.meinders@ctw.utwente.nl
2. Email: n.verdonschot@orthop.umcn.nl
3. Email: e.tanck@orthop.umcn.nl

References

Bayraktar HH, Gupta A, Kwon RY, Papadopoulos P, Keaveny TM. 2004. The modified super-ellipsoid yield criterion for human trabecular bone. J Biomech Eng. 126(6): 677–684.

Bayraktar HH, Morgan EF, Niebur GL, Morris GE, Wong EK, Keaveny TM. 2004. Comparison of the elastic and yield properties of human femoral trabecular and cortical bone tissue. J Biomech. 37(1):27–35.

Bessho M, Ohnishi I, Matsumoto T, Ohashi S, Matsuyama J, Tobita K, Kaneko M, Nakamura K. 2009. Prediction of proximal femur strength using a CT-based nonlinear finite element method: differences in predicted fracture load and site with changing load and boundary conditions. Bone. 45(2):226–231.

Bessho M, Ohnishi I, Matsuyama J, Matsumoto T, Imai K, Nakamura K. 2007. Prediction of strength and strain of the proximal femur by a CT-based finite element method. J Biomech. 40(8):1745–1753.

Body JJ. 2003. Rationale for the use of bisphosphonates in osteoblastic and osteolytic bone lesions. Breast. 12(Suppl 2): S37–S44.

Harvey HA. 1997. Issues concerning the role of chemotherapy and hormonal therapy of bone metastases from breast carcinoma. Cancer. 80(Suppl 8):1646–1651.

Hipp JA, Springfield DS, Hayes WC. 1995. Predicting pathologic fracture risk in the management of metastatic bone defects. Clin Orthop Relat Res. 312:120–135.

Hoskin PJ. 2003. Bisphosphonates and radiation therapy for palliation of metastatic bone disease. Cancer Treat Rev. 29(4):321–327.

Kaneko TS, Pejcic MR, Tehranzadeh J, Keyak JH. 2003. Relationships between material properties and CT scan data of cortical bone with and without metastatic lesions. Med Eng Phys. 25(6):445–454.

Keaveny TM, Wachtel EF, Ford CM, Hayes WC. 1994. Differences between the tensile and compressive strengths of bovine tibial trabecular bone depend on modulus. J Biomech. 27(9):1137–1146.

Keyak JH. 2001. Improved prediction of proximal femoral fracture load using nonlinear finite element models. Med Eng Phys. 23(3):165–173.

Keyak JH, Kaneko TS, Rossi SA, Pejcic MR, Tehranzadeh J, Skinner HB. 2005. Predicting the strength of femoral shafts with and without metastatic lesions. Clin Orthop Relat Res. 439:161–170.

Keyak JH, Kaneko TS, Skinner HB, Hoang BH. 2007. The effect of simulated metastatic lytic lesions on proximal femoral strength. Clin Orthop Relat Res. 459:139–145.

Keyak JH, Kaneko TS, Tehranzadeh J, Skinner HB. 2005. Predicting proximal femoral strength using structural engineering models. Clin Orthop Relat Res. 437:219–228.

Keyak JH, Rossi SA. 2000. Prediction of femoral fracture load using finite element models: an examination of stress- and strain-based failure theories. J Biomech. 33(2):209–214.

Kopperdahl DL, Keaveny TM. 1998. Yield strain behavior of trabecular bone. J Biomech. 31(7):601–608.

Kyle RF, Cabanela ME, Russell TA, Swiontkowski MF, Winquist RA, Zuckerman JD, Schmidt AH, Koval KJ. 1995. Fractures of the proximal part of the femur. Instr Course Lect. 44:227–253.

Lenaerts L, van Lenthe GH. 2009. Multi-level patient-specific modelling of the proximal femur. A promising tool to quantify the effect of osteoporosis treatment. Philos Transact A Math Phys Eng Sci. 367(1895):2079–2093.

Mirels H. 1989. Metastatic disease in long bones. A proposed scoring system for diagnosing impending pathologic fractures. Clin Orthop Relat Res. 249:256–264.

Morgan EF, Keaveny TM. 2001. Dependence of yield strain of human trabecular bone on anatomic site. J Biomech. 34(5): 569–577.

Mullins LP, Bruzzi MS, McHugh PE. 2009. Calibration of a constitutive model for the post-yield behaviour of cortical bone. J Mech Behav Biomed Mater. 2(5):460–470.

Niebur GL, Feldstein MJ, Yuen JC, Chen TJ, Keaveny TM. 2000. High-resolution finite element models with tissue strength asymmetry accurately predict failure of trabecular bone. J Biomech. 33(12):1575–1583.

Orwoll ES, Marshall LM, Nielson CM, Cummings SR, Lapidus J, Cauley JA, Ensrud K, Lane N, Hoffmann PR, Kopperdahl DL, Keaveny TM. 2009. Finite element analysis of the proximal femur and hip fracture risk in older men. J Bone Miner Res. 24(3):475–483.

Tanck E, van Aken JB, Van der Linden YM, Schreuder HW, Binkowski M, Huizenga H, Verdonschot N. 2009. Pathological fracture prediction in patients with metastatic lesions can be improved with quantitative computed tomography based computer models. Bone. 45(4):777–783.

Van der Linden YM, Dijkstra PD, Kroon HM, Lok JJ, Noordijk EM, Leer JW, Marijnen CA. 2004. Comparative analysis of risk factors for pathological fracture with femoral metastases. J Bone Joint Surg Br. 86(4):566–573.

Van der Linden YM, Kroon HM, Dijkstra SP, Lok JJ, Noordijk EM, Leer JW, Marijnen CA. 2003. Simple radiographic parameter predicts fracturing in metastatic femoral bone lesions: results from a randomised trial. Radiother Oncol. 69(1):21–31.